future pharmacology

MDPI

Article

Modulation of *Staphylococcus aureus* Biofilm Formation through Subinhibitory Concentrations of Biogenic Silver Nanoparticles and Simvastatin

Ana Carolina Furian da Silva [1], Sindy Magri Roque [1], Marta Cristina Teixeira Duarte [2], Gerson Nakazato [3], Nelson Durán [4] and Karina Cogo-Müller [1,*]

[1] Laboratory of Pharmacology of Antimicrobials and Microbiology, Faculty of Pharmaceutical Sciences, Universidade Estadual de Campinas (UNICAMP), Campinas 13083-871, SP, Brazil; a210740@dac.unicamp.br (A.C.F.d.S.); s152591@dac.unicamp.br (S.M.R.)
[2] Laboratory of Microbiology, Pluridisciplinary Center for Chemical, Biological and Agricultural Research, Universidade Estadual de Campinas (UNICAMP), Campinas 13148-218, SP, Brazil; mduarte@cpqba.unicamp.br
[3] Department of Microbiology, Center of Biological Sciences, University of Londrina (UEL), Londrina 86057-970, PR, Brazil; gnakazato@uel.br
[4] Laboratory of Urogenital Carcinogenesis and Immunotherapy, Universidade Estadual de Campinas (UNICAMP), Campinas 13083-970, SP, Brazil; nduran@g.unicamp.br
* Correspondence: author: karinacm@unicamp.br

Abstract: *Staphylococcus aureus* is a causative agent of nosocomial infections and its antibiotic-resistant strains give cause for concern. Solutions are being explored to improve treatment for these infections, including repositioning drugs such as statins and using nanoparticles with antimicrobial properties. This study evaluated the antimicrobial effects of simvastatin (SIM) and biologically synthesized silver nanoparticles (bio-AgNPs) in isolate form and in combination using assays of minimum inhibitory concentration (MIC), an in vitro biofilm model, and the association of antimicrobials against clinical strains of *S. aureus*. Bio-AgNPs showed a 53.8 ± 1.23 nm mean diameter and standard deviation, a 0.23 polydispersity index, and a −25.66 ± 2.19 mV mean potential and standard deviation. Transmission electron microscopy confirmed the formation of nanoparticles, and the presence of Ag0 and AgCl. *S. aureus* strains were sensitive to bio-AgNPs and SIM, showing 31.88–187.5 and 74.66–149.32 µM concentrations, respectively. The association assay showed 2.0 fractional inhibitory concentration indices (i.e., indifferent for clinical strains) and 0.32 values for the standard ATCC 29213 strain (synergy). Biofilm inhibition assays with isolated SIM and bio-AgNPs showed decreased biofilm formation 4× to 1/8 MICs concentrations, showing no synergism in association. These findings evince that simvastatin and bio-AgNPs at subinhibitory concentrations can serve as antimicrobial agents against *S. aureus* biofilm.

Keywords: *Staphylococcus aureus*; statins; biofilm; antimicrobials; silver nanoparticle

Citation: da Silva, A.C.F.; Roque, S.M.; Duarte, M.C.T.; Nakazato, G.; Durán, N.; Cogo-Müller, K. Modulation of *Staphylococcus aureus* Biofilm Formation through Subinhibitory Concentrations of Biogenic Silver Nanoparticles and Simvastatin. *Future Pharmacol.* **2024**, *4*, 3–16. https://doi.org/10.3390/futurepharmacol4010002

Academic Editor: Karol Wróblewski

Received: 23 October 2023
Revised: 8 December 2023
Accepted: 2 January 2024
Published: 5 January 2024

1. Introduction

Staphylococcus aureus is one of the most important bacteria agents in nosocomial infections, whose antibiotic-resistant or non-susceptible strains (including to vancomycin, daptomycin, and ceftaroline) cause increasing concern [1,2]. Methicillin-resistant *Staphylococcus aureus* (MRSA) stands out among the most prevalent resistant strains. WHO 2020 global data showed a 24.9% average of infection cases by MRSA [3]. *Staphylococcus aureus* can cause skin and soft tissue infections [1,4] (including those in catheters and prosthetic devices), implant-associated infections, bacteremia, endocarditis, osteomyelitis, and pneumonia, among others [1].

MecA is a crucial gene that provides MRSA with the inherent ability to grow in the presence of penicillin-like antibiotics. Present in all MRSA strains, this gene codes for

penicillin-binding protein 2a (PBP2a) [5]. PBPs are enzymes located on the cell membrane and serve essential functions in microbial growth, cell division, and cell structure [6]. Further compounding the problem is the fact that MRSA has a high capacity to form biofilms on biotic and abiotic surfaces [7–9], biological communities that are believed to account for nearly 80% of all human infections. Moreover, one of their most significant attributes is their high resistance to antibiotics, disinfectants, host immune defenses, and environmental stress [10,11].

Solving these problems requires searching for and developing new antibacterial compounds. Metallic nanoparticles offer a possible antimicrobial agent. As many studies have shown, silver nanoparticles (AgNP) have a synergistic effect with other clinically used antibiotics and even other antimicrobial substances [12,13]. These associations between AgNP and antimicrobial drugs can direct the latter towards specific targets and boost their effect by decreasing antimicrobial resistance [12,14].

The great advantage of synthesizing AgNP is the possibility of producing them from the biogenic-sourcing processes—plant extracts or microorganisms (green synthesis)—which are usually easy to perform, economically viable, secure, and scalable [15]. The fungus *Fusarium oxysporum* is one of the microorganisms that can produce silver nanoparticles. Its production methodology consists of adding silver nitrate ($AgNO_3$) to a fungal extract, which, by the action of reducing enzymes such as nitrate reductase, will reduce the silver and synthesize silver nanoparticles, attested by the color change of the extract to a yellowish-brown [16,17].

Repositioning drugs that show antimicrobial activity as a side effect is an alternative against antibiotic-resistant strains [18]. Drug associations can also produce synergism, as some drugs tested under a monotherapy regimen fail to show significant antibacterial activity but are effective when associated with antibiotics, considerably reducing their dose [19–21].

Considered one of the most prescribed drugs in the world, with up to 200 million people worldwide using them daily [22], statins are important lipid-lowering agents (exerting their effect by inhibiting the enzyme 3-hydroxy-3methyl-glutaryl-Coenzyme-A reductase—HMG-CoA), leading to a decreased synthesis of cholesterol and low-density lipoproteins circulating in the body. When administered orally, these drugs are well tolerated; however, some patients might experience severe adverse effects like instances of muscle toxicity, leading to rare conditions such as rhabdomyolysis and myopathy [23–25].

Studies have evaluated the effects of statins (called pleiotropic effects) besides lowering cholesterol, highlighting their antioxidant [26], anticarcinogenic [27], anticoagulant [28], anti-inflammatory [29], and immunomodulating effects [30].

An effect that has gained increasing prominence is their antimicrobial effect, especially that of simvastatin (SIM), shown to have antimicrobial activity against *S. aureus* in both planktonic growth and biofilm [31,32]. Simvastatin can also reduce the formation of multispecies biofilms and possibly treat oral infections [33,34].

AgNP associated with SIM has already been shown to be synergistic against standard and resistant strains of *S. aureus* [17]. In isolation, studies show that both compounds act against *S. aureus* biofilm [32,35–37], but no study has evaluated a possible synergistic interaction between these drugs against MRSA biofilm. *S. aureus* biofilm formation in the clinical environment mainly affects the surfaces of implanted catheters and medical devices, requiring their replacement with new ones and the use of oral antibiotics as treatment, drastically increasing cure costs and time (which may span up to six months or more) [38,39]. Thus, this study evaluated the pharmacological interaction between simvastatin and AgNP in an in vitro biofilm model, suggesting a future alternative as an adjuvant treatment to *S. aureus* bacterial biofilm.

2. Materials and Methods

2.1. Substances and Experimental Groups

Bio-AgNP (3 mM) and SIM (EMS, Pharmaceutical Industry, São Paulo, Brazil) suspensions were used for the antimicrobial activity assays. The bio-AgNP suspension was diluted in sterile water and the SIM in DMSO (Dimethylsulfoxide). The highest tested SIM concentration (597.2 µM) with 2.5% DMSO was found to be non-toxic to bacterial cultures.

2.1.1. Bio-AgNP Synthesis

Bio-AgNPs were synthesized according to Durán et al. [16] (Patent, 2006, PI 0605681-4A2 [40]; http://www.inpi.gov.br, accessed on 10 October 2023). Bio-AgNPs were prepared using a silver nitrate reduction catalyzed with a cell-free enzyme preparation of *F. oxysporum* (strain 551) from a culture collected at the Molecular Genetics Laboratory (Universidade de São Paulo, ESALQ, Piracicaba, Brazil) [16,41]. The fungus was cultured in an agar medium containing 0.5% yeast extract (BD, Franklin Lakes, NJ, USA), 2% malt extract (BD), and 2% agar (BD) and incubated at 28 °C for seven days. After fungus growth, the produced biomass was added to sterile distilled water (0.1 g/mL) under agitation at 150 rpm (Agitator Tecnal, Piracicaba, SP, Brazil) for 72 h. After vacuum filtration, 0.01 mol/L of silver nitrate ($AgNO_3$, Nuclear, São Paulo, SP, Brazil) was added to the supernatant (Filtrate fungal—FF) and protected from light.

2.1.2. Bio-AgNP Characterization

Hydrodynamic radius, zeta potential, and polydispersion index (PDI) of the bio-AgNPs were determined with dynamic light scattering using ZetaSizer NanoZS (Malvern Panalytical®, Malvern, UK). AgNP morphology and size were confirmed using transmission electron microscopy (TEM) performed using JEM-1400Plus (Jeol®, Akishima, Japan). Particle size was determined using dynamic light scattering (DLS).

2.1.3. Bio-AgNP and Simvastatin Antimicrobial Activity

Bio-AgNPs and SIM antimicrobial activity was investigated using microdilution and antimicrobial combination assay against *S. aureus* strains. Biofilm inhibition was evaluated through assays, both individually and in combination.

2.1.4. Bacteria and Growing Conditions

The following microorganism strains were used: methicillin-resistant *S. aureus* (MRSA) strains isolated from sputum samples (HC 3817719, 10106876, and 9120358); methicillin-susceptible *S. aureus* (MSSA) strains from blood cultures (HC 12092392, 985444, 909, 1734, 1744, and 1641); and standard *S. aureus* strains (ATCC 43300, 33591, 29213, and ATCC 6538). The strains were kindly provided by Professor Carlos Emilio Levy of the School of Medical Sciences, Department of Clinical Pathology, University of Campinas, Brazil. The cultures were stored in a tryptic soy broth medium (TSB-Difco Co., Detroit, MI, USA) with 20% glycerol (Sigma-Aldrich, St. Louis, MO, USA) at −80 °C. The bacteria were cultured in a tryptic soy agar medium (TSA, Difco Co., Detroit, MI, USA) and incubated in aerobiosis.

2.1.5. Minimum Inhibitory Concentration (MIC) Assay

MIC was conducted following the Clinical and Laboratory Standards Institute recommendations [42]. The assays were performed using 96-well plates and Mueller Hinton broth (MHB, Difco Co., Detroit, MI, USA). Concentrations ranging from 597.2 to 0.28 µM for SIM and from 750 to 0.36 µM for AgNP were serially diluted in 100 µL of MHB per well plate. Bacteria were reactivated and cultured in TSA for 24 h at 35 °C. From the grown cultures, a microbial suspension was prepared until it reached a 0.1 absorbance under a 660 nm wavelength, resulting in a concentration of 1×10^8 CFU/mL. A diluted suspension was then prepared using a reservoir with 9.9 mL of MHB medium and 100 µL of bacterial inoculum (1×10^6 CFU/mL final concentration). Finally, 100 µL of the dilution was added to each plate well, reaching a final concentration of 5×10^5 CFU/well. The plates were

incubated for 24 h at 35 °C and visually analyzed for turbidity, whereas absorbance was assessed in a spectrophotometer (ƛ = 660 nm). Moreover, 30 µL of resazurin dye 0.01% (Inlab, Diadema, SP, Brazil) was added to each well. Plates were then incubated for two hours and visually inspected to confirm the results obtained.

2.1.6. Antimicrobial Combination Assay

A microdilution association method was used to evaluate the possible interaction between bio-AgNPs and SIM [32,43]. In it, dilutions with different concentrations of each substance, using the MIC assay concentration as reference, were associated in two directions (vertical and/or horizontal) and prepared in 100 µL of MHB broth across the 96 wells. Strains were cultured and a suspension was prepared according to previous description (MIC assay). A 100 µL aliquot of the bacterial suspension in each well was used with a final 5×10^5 CFU/well concentration. The plates were then incubated for 24 h at 35 °C in aerobiosis and visually analyzed for turbidity, whereas absorbance was assessed using a spectrophotometer (ƛ = 660 nm). Finally, 30 µL of resazurin dye (0.01% solution in water) was added to each well, which was incubated for two hours and visually verified. Results were analyzed using their fractional inhibitory concentration index (FICI) values, calculated as follows: Σ = FICIA + FICIB = MICAB/MICA + MICBA/MICB, in which MIC A and B denote the concentrations for individual substances, whereas MIC AB and BA represent the concentrations of A and B combined. FICI values < 0.5 synergism; those between 0.5 and 1.0, an additive effect; those between 1.0 and 4.0, indifference; and those >4, antagonism [44].

2.1.7. Biofilm Formation Inhibition Assay

Prior to this assay, the biofilm-forming capacity of all bacterial strains was assessed. Among them, the HC 3817719 (MRSA), 10106876 (MRSA), 9120358 (MRSA), 1734 (MSSA), 909 (MSSA), and 12092392 (MSSA) strains showed the highest biofilm formation capacity. For the assay, 96-well U-bottom plates were used and concentrations of 4× to 1/8 MIC were chosen as the study SIM and Bio-AgNP range. The assay was performed as previously described [32]. Bacteria were reactivated and cultured in TSA for 24 h at 35 °C. Serial dilutions (2×) of SIM and Bio-AgNP were prepared in 100 µL TSB supplemented with 1% glucose (Labsynth, Diadema, São Paulo, Brazil) in each well. A bacterial suspension was prepared and diluted until it reached a 0.1 absorbance (wavelength of 660 nm). Then, 100 µL of the previously diluted suspension was added to each well (50 µL of suspension in 10 mL of TSB medium supplemented with 1% glucose and 100 µL of the culture medium). After 24 h of incubation at 35 °C, the plates were removed and the biofilm was gently washed with deionized distilled water to remove non-adherent cells. The wells were allowed to dry at room temperature and optical density measurements (540 nm) were performed to quantify the biofilm formed after incubation with 0.4% crystal violet solution and 100% ethanol for 30 min [45].

2.2. Statistical Analyses

Data distribution was verified using the Shapiro–Wilk test and homoscedasticity, by Levene's test. Data were compared with the control group using analysis of variance (ANOVA) and Tukey's post-test. All analyses were performed using Bioestat 5.0 (Mamirauá, Belém, Brazil) and GraphPad Prism 8.0 (GraphPad, San Diego, CA, USA). A 0.05% significance level was established.

3. Results

3.1. Bio-AgNP Characterization

We evaluated nanoparticle diameter using DLS. Bio-AgNPs showed a 53.8 ± 1.23 nm mean diameter and standard deviation, a 0.23 polydispersity index, and a -25.66 ± -2.19 mV mean potential and standard deviation. Thus, the nanoparticles showed dispersion and homogeneous distribution.

Figure 1 represents the nanoparticles evaluated using transmission electron microscopy (TEM). We found spherical and homogeneous nanoparticles dispersed in the suspension.

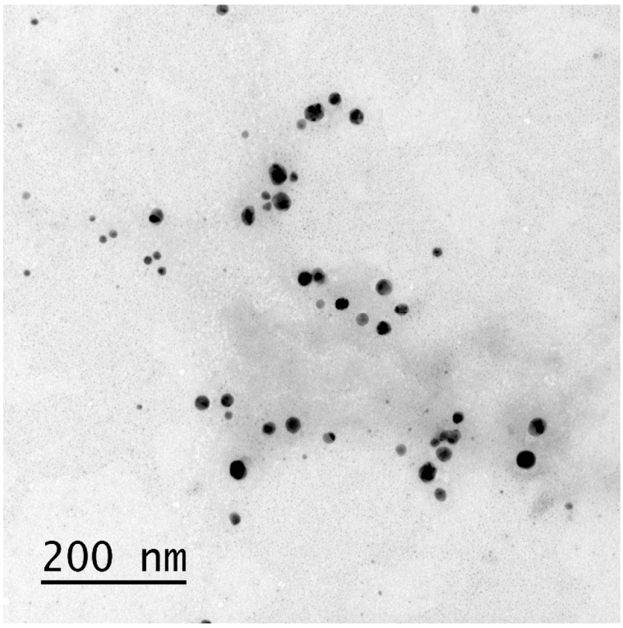

Figure 1. Characterization using transmission electron microscopy (TEM) of bio-AgNP suspensions synthesized with *F. oxysporum* and deposited in a copper sample port coated with parlodium film at 200 nm.

3.2. Minimum Inhibitory Concentration (MIC) and Antimicrobial Combination (FICI) Assays

SIM showed inhibitory activity at low concentrations in all nine clinical strains. For most strains, MICs' values ranged from 74.66 to 149.32 µM (Table 1). Bio-AgNPs showed inhibitory activity at concentrations above SIM, from 31.88 to 187.5 µM (Table 1). Use of DMSO as a solvent at low concentrations (2.5% at the highest concentration) showed no difference compared with the positive control (water), indicating that the vehicle used failed to interfere with the simvastatin activity.

Table 1. Minimum inhibitory concentration (MIC), antimicrobial association, and fractionated inhibitory concentration (FICI) for *S. aureus* strains. Concentrations expressed in µM.

Strains	MIC		Association MIC	FICI Index
	SIM (µM)	Bio-AgNP (µM)	SIM + Bio-AgNP	
S. aureus ATCC 29213	74.66	31.88	74.66 + 31.88	0.32
S. aureus ATCC 43300	149.32	63.75	149.32 + 63.75	2.0
S. aureus ATCC 33591	149.32	31.88	149.32 + 31.88	2.0
S. aureus ATCC 6538	74.66	31.88	74.66 + 31.88	2.0
S. aureus HC 3817719 (MRSA)	74.66	187.5	74.66 + 187.5	2.0
S. aureus HC 10106876 (MRSA)	74.66	187.5	74.66 + 187.5	2.0
S. aureus HC 9120358 (MRSA)	74.66	187.5	74.66 + 187.5	2.0
S. aureus HC 12092392 (MSSA)	74.66	93.75	74.66 + 93.7	2.0
S. aureus HC 985444 (MSSA)	74.66	93.75	74.66 + 93.75	2.0
S. aureus 909 (MSSA)	149.32	187.5	149.32 + 187.5	2.0
S. aureus 1734 (MSSA)	74.66	93.75	74.66 + 93.75	2.0
S. aureus 1744 (MSSA)	74.66	187.5	74.66 + 187.5	2.0
S. aureus 1641 (MSSA)	74.66	187.5	74.66 + 187.5	2.0

In association, bio-AgNPs and simvastatin showed equal MIC values to the isolated compounds, resulting in a 2.0 FICI indifferent association (Table 1).

3.3. Biofilm-Formation-Inhibition Assay

This assay tested the ability of SIM and bio-AgNPs (alone and in association) to inhibit biofilm formation at concentrations ranging from 4× to 1/8MIC, i.e., from 9.31 to 597.2 µM and from 11.7 to 750 µM for simvastatin and AgNP, respectively. Figures 2–4 show the optical density readings of biofilm formation in 96-well plates stained with violet crystal after 24 h of formation for the ATCC 29213, MSSA, and MRSA strains, respectively. Overall, SIM and bio-AgNPs inhibited biofilm formation 4× to 1/8 MIC concentrations for almost all strains ($p < 0.05$, ANOVA, Tukey) when compared with the control group. Results for isolated AgNP evince that the MRSA HC 3817719 strain showed a slight increase in bacterial growth in relation to control, with statistical differences in 1/4 and 1/8 MIC concentrations. We observed the same profile for the HC 9120358 strain at the 1/8 MIC concentration, although statistically indifferent.

Bio-AgNP and SIM association also inhibited biofilm with a profile similar to those for isolated substances, showing inhibition at concentrations from 4× to 1/8 MIC. When in association, the 2× MIC concentration for the MSSA HC 909 strain showed a higher growth profile than the control, but without statistical differences. For the MRSA HC 3817719 strain, the 1/8 MIC concentration showed a statistical difference ($p > 0.05$, ANOVA, Tukey).

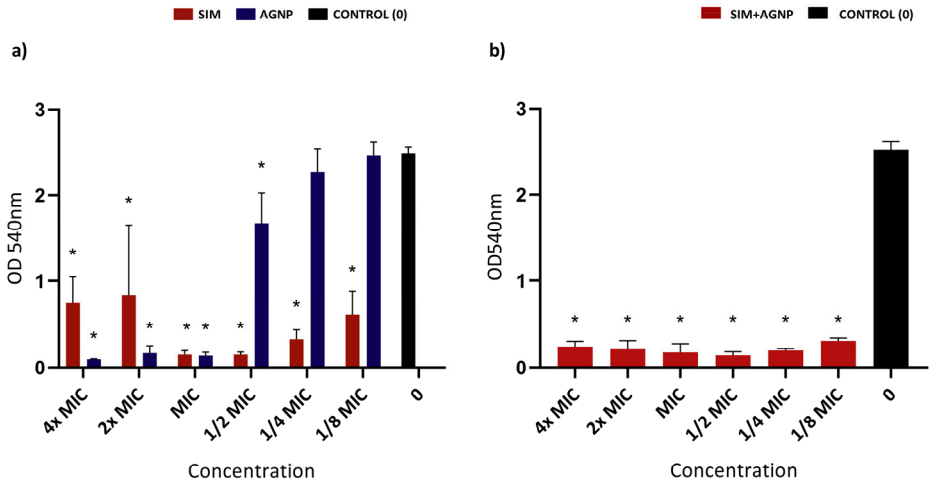

Figure 2. Graph (**a**) represents biofilm inhibition for SIM and bio-AgNP and graph (**b**) represents biofilm inhibition by association at concentrations from 4× to 1/8 MIC for the standard *S. aureus* ATCC 29213 strain after 24 h. The expressed values refer to the mean and standard deviation of the absorbance readings (OD 540 nm). * indicates statistical differences from the control. (ANOVA, 2 criteria, Tukey). Column "0" indicates the growth of the untreated standard ATCC 29213 strain.

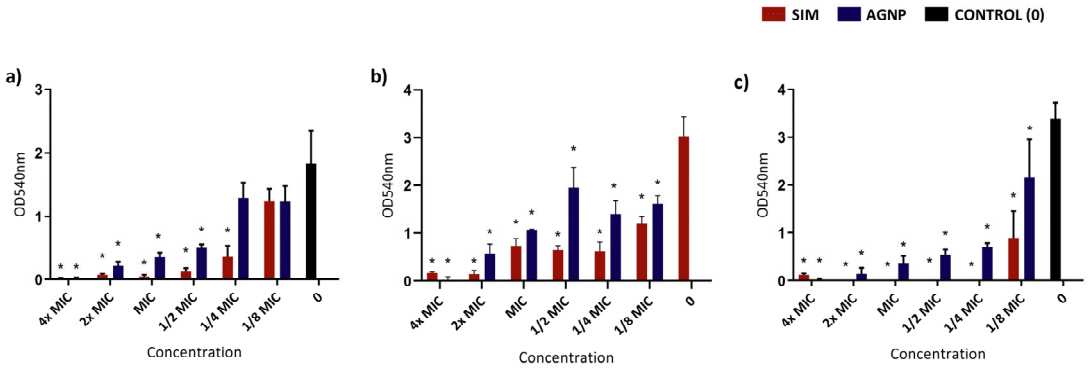

Figure 3. *Cont.*

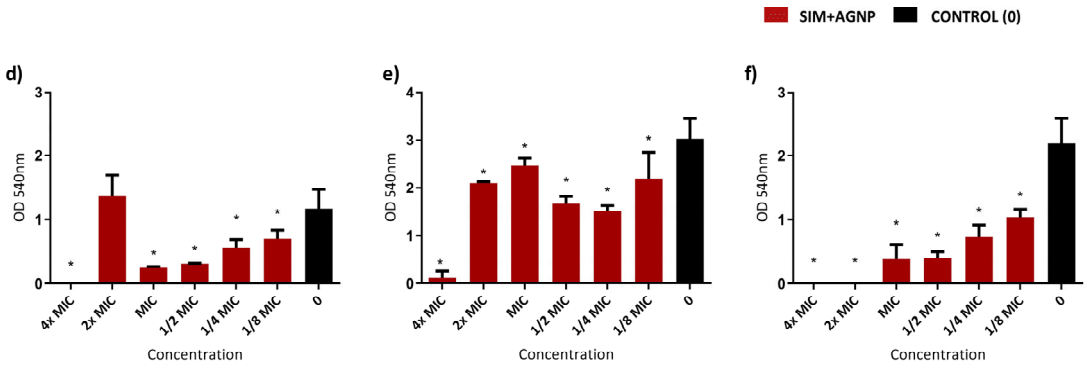

Figure 3. Graphs (**a**–**c**) represent biofilm inhibition for SIM and bio-AgNP at concentrations from 4× to 1/8 MIC for methicillin-sensitive *S. aureus* 909, 1734 and 12092392 strains (MSSA) after 24 h. Graphs (**d**–**f**) represent biofilm inhibition by association for the same MSSA strains after 24 h. Values expressed are the mean and standard deviation of the absorbance readings (OD 540 nm). * indicates statistical differences from the control. (ANOVA, 2 criteria, Tukey). Column "0" indicates bacterial growth without treatment.

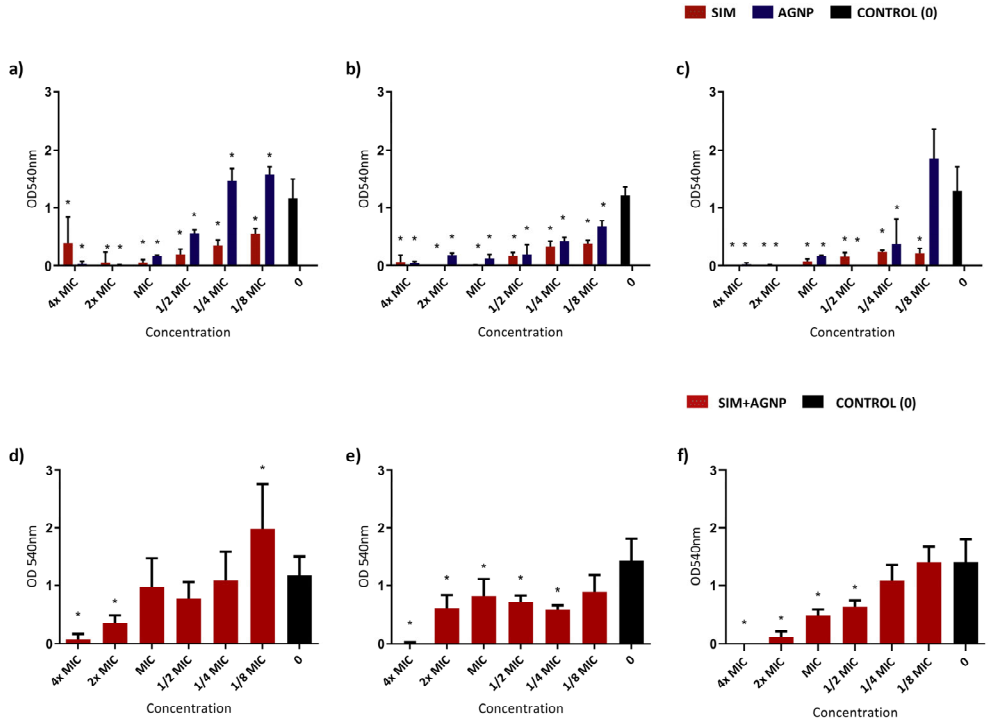

Figure 4. Graphs (**a**–**c**) represent biofilm inhibition for SIM and bio-AgNP at concentrations from 4× to 1/8 MIC for methicillin-resistant *S. aureus* 3817719, 10106876 and 9120358 (MRSA) strains after 24 h. Graphs (**d**–**f**) represent biofilm inhibition by association for the same MRSA strains after 24 h. Values expressed are the mean and standard deviation of the absorbance readings (OD 540 nm). * indicates statistical differences from the control. (ANOVA, 2 criteria, Tukey). Column "0" indicates bacterial growth without treatment.

4. Discussion

Staphylococcus aureus is a Gram-positive bacterium often found in nosocomial infections that may resist antibiotics and complicate treatment [1,2]. Drug repositioning may configure a promising approach to treating infections, especially in the face of growing microbial resistance [18]. Statins (especially simvastatin) have been studied for their antimicrobial potential, especially against *S. aureus* [30]. Moreover, the use of silver nanoparticles as a topical agent in wounds or medical materials has been investigated to control *S. aureus*

biofilm [31,32]. This study produced and characterized bio-AgNPs, testing them in isolation and in association with simvastatin against clinical strains of *S. aureus*. Both substances showed antimicrobial activity at subinhibitory concentrations, reducing *S. aureus* biofilm formation. When associated, they showed synergism only for the standard *S. aureus* strain, with no change in activity against clinical MRSA and MSSA strains. We prepared our silver nanoparticles by biologically obtaining metallic nanoparticles from fungi [16], which have greater advantages over chemical and physical methods. Fungi are easy to grow, can occupy large surface areas, and facilitate nanoparticle synthesis due to their easy biomass manipulation [46,47]. Fungal mycelia exhibit a superior ability to withstand high-flow pressure, agitation, and other challenging conditions encountered in bioreactions in comparison to other microbes and plants [48] and enable cost-effective large-scale synthesis, requiring only a minimal quantity of biomass [49]. Moreover, they neither harm the environment nor require toxic chemicals or radiation [15]. The obtained bio-AgNPs had adequate size (below 100 nm) and good polydispersity and zeta potential indices, as observed in previous studies using biogenic production [16]. The diameter observed in TEM images showed smaller particles according to our distribution histogram (5–30 nm). This stems from the fact that the DLS measures hydrodynamic radii, i.e., it considers particles and the stabilization layers around them—the protein layer from the synthesis of the fungal filtrate [16]. Bio-AgNPs showed a -25.66 ± 2.19 mV zeta potential, corroborating Raj et al. [50]. A negative zeta potential indicates the predominance of particles with surface electric charges, contributing to the repulsion between nanoparticles, reducing aggregation, and increasing their stability [51].

Both bio-AgNPs and simvastatin have shown antimicrobial activity against opportunistic pathogens and oral-cavity bacteria [22,32,52]. SIM and bio-AgNP minimum-inhibitory-concentration assays showed good antimicrobial activity, inhibiting the bacterial growth of all *S. aureus* strains in concentrations from 74.66 to 37.27 μM (SIM) and from 187.5 to 93.75 μM (bio-AgNP). Our research group previously found similar MIC values for SIM [32]. For the bio-AgNPs tested against *S. aureus*, we found MIC values in the same range as in this study [17,32,53]. When tested against clinical strains of *Pseudomonas aeruginosa*, bio-AgNPs showed an inhibitory concentration comparable to the one in this study (62.5 μM) [54].

According to FICI, association assays showed no synergistic effect against the clinical strains of *S. aureus*, unlike that for the ATCC 29213 strain, which resulted in a synergistic effect. Figueiredo et al. found the same synergistic result against a standard (ATCC 25923) and an MRSA strain (MRSA N315) [17]. Thus, for standard *S. aureus* strains, the association of bio-AgNP and SIM can promote a synergistic effect, which is rare for clinical strains isolated from patients. Therefore, the use of these substances for clinical use may fail to offer additional benefits when compared to isolated products.

Such difference in results may be attributed to variations in the lipid profile of the standard and clinical strain. Using gas chromatography coupled with mass spectrometry analysis, one study highlighted qualitative and quantitative differences in the bacterial lipid profiles of ATCC and clinical strains of *S. aureus*, which impacted both antibiotic resistance and surface hydrophobicity. Resistance may also be related to the source of infection from which the strains were isolated, reflecting their potential capacity to create biofilm [55]. In the case of ATCC strains, natural genetic variation may be a crucial factor in its response to antimicrobial agents.

Other studies have found synergism between antibiotics and silver nanoparticles. Habash et al. found that AgNP coated with 10 and 20 nm of citrate boosted the effect of tobramycin in both planktonic cultures and *P. aeruginosa*-strain biofilm [56]. AgNP averaging 45 nm in size (from the aqueous extract of *Zea mays* leaf residues) showed synergistic activity against *Bacillus cereus*, *Escherichia coli*, *Listeria monocytogenes*, *S. aureus*, and *Salmonella typhimurium* when associated with antibiotics such as kanamycin and rifampicin B [13]. Based on these findings, our research group conducted studies associating

simvastatin with silver nanoparticles. We then found synergism in standard strains but not in clinically isolated strains, as described here.

When testing the capacity of isolated substances to inhibit biofilm formation, in general, concentrations of 1/8 and 1/4 MIC for SIM and bio-AgNP showed no inhibition. In most strains, subinhibitory concentrations ($^1/_2$ and 1/4 MIC) were sufficient to inhibit biofilm formation for SIM and AgNP in comparison to the control group (no treatment). For HC 3817719 (a resistant strain), we obtained a biofilm growth increase greater than the control in 1/8 and 1/4 MIC concentrations (isolated bio-AgNPs) and in the 1/8 concentration (association). Other studies have shown increased biofilm in subinhibitory bio-AgNP concentrations, when compared to other bacterial genera [54,57]. Such increases can be attributed to AgNPs inducing the generation of reactive oxygen species (ROS), resulting in oxidative stress [58]. ROS can cause detrimental alterations to cellular components and harm proteins, DNA, and lipids [59]. Increased oxidative stress likely exerted selective pressure at the early stages of biofilm development, increasing its formation capacity [57].

Using subinhibitory concentrations of antimicrobial agents offers many advantages, including a potential reduction in antimicrobial-resistance development due to reduced selective pressure [60]. It also aids in inhibiting biofilm formation by disrupting the extracellular matrix, as well as reducing surface adhesion and aggregation of surviving cells [32]. Combining treatments enhances antimicrobial effects and provides a more comprehensive approach to biofilm inhibition [58,61], while concurrently reducing toxicity to host cells and minimizing the adverse effects on surrounding tissues [62]. Moreover, it helps to prevent recurrent infections, thereby improving long-term treatment effectiveness [63]. Notably, use of subinhibitory concentrations potentially leads to resource savings by reducing the total antimicrobial requirement, optimizing resource utilization and mitigating the risk of side effects associated with higher doses.

Importantly, reports on antimicrobial resistance to AgNPs or even to simvastatin are scarce [22,64], increasing interest in possibly using these substances as they exhibit antibiofilm effects even at subinhibitory concentrations.

Combined substances showed no greater effect on biofilm inhibition than isolated substances. In standard *S. aureus* strains, despite the synergistic nature observed in association tests, the combined use of SIM and bio-AgNP did not amplify their antibiofilm effect in comparison to their isolated use. In *Arpergillus* biofilm, inhibition by associating bio-AgNP and simvastatin at concentrations from 2× to 8× MIC also resembled isolated substances [65]. This study found a synergistic effect between bio-AgNP and SIM when tested in fungi in its association assay. So, despite the synergism between substances in association assays, when tested on biofilm, the inhibition profile of the association remained similar to that of isolated substances [65].

AgNPs-based medical devices have been greatly explored, such as different-type catheters (glass, plastic, polyurethane), for their effectiveness in antibacterial and antibiofilm applications [66]. Plastic and polyurethane catheters implanted with AgNPs significantly reduced infection rates and prevented multispecies biofilm formation [67–69]. A study on hemodialysis catheters found that using polyurethane catheters for vascular access and blood filtration causes infections that often lead to patients' death, but photochemically depositing AgNPs at the infection site inhibited bacterial growth. The developed surface coating can produce safe, cost-effective catheters with low infection rates [70].

Toxicity of silver ions is questionable, but some studies have shown that incorporating them into nanoparticles decreases their cytotoxicity. Using cell culture assays, bio-AgNP showed no cytotoxicity against immune cells (T, B, and NK cells) from 3 to 72 h of exposure [71,72]. In contact with mouse (Balb/c)-skin fibroblasts, exposure to bio-AgNP preserved cellular structures, a result seen on TEM images of IC20 nontoxic concentrations (91.77 μg/mL) [73,74].

Statins, especially in combination with AgNPs, present an interesting use for topical application or even in coating medical devices such as implants, probes, and catheters [75]. Some studies have proposed coating medical devices with AgNPs to reduce microbial

adhesion, thus preventing nosocomial infections. As for topical use, application would be beneficial in treating topical skin infections, especially those caused by *S. aureus*. Local application of SIM and AgNPs could ensure concentrations above the MIC at the affected site, while also reducing potential systemic adverse events, such as rhabdomyolysis [24,25]. Further studies are needed to verify the safety and toxicity of this association, as statins can generate adverse reactions such as cheilitis [76], autoimmune inflammatory syndromes similar to dermatomyositis and lupus [77,78], phototoxicity [79], and occupational contact dermatitis [80,81], among others [82–84]. However, the risk of adverse cutaneous reactions seems to be relatively low [78].

Thus, based on our data, we conclude that the association of SIM and bio-AgNP performs no better than isolated substances in clinical strains of *S. aureus*. Clinically, the association may be interesting to treat or prevent biofilm formation/infections from more than one bacterial species since their sensitivity to each substance may differ, thus increasing their spectrum of action. For this, further studies with other bacterial species should be conducted to evaluate the possible interaction between these substances and the relevance of their associated clinical use.

5. Conclusions

Our findings evince that SIM and bio-AgNP have antimicrobial activity at subinhibitory concentrations and may be used in hospitals (impregnated in materials and to treat wound and burn infections). Although not synergistic, these compounds maintained antimicrobial activity when associated in suspension and biofilm. Further studies are needed to evaluate the clinical relevance and mechanisms of the antimicrobial action of these substances in association.

Author Contributions: Conceptualization, K.C.-M. and N.D.; methodology, K.C.-M., N.D., A.C.F.d.S. and S.M.R.; software, K.C.-M., A.C.F.d.S., S.M.R. and M.C.T.D.; validation, A.C.F.d.S. and S.M.R.; investigation, K.C.-M., A.C.F.d.S. and S.M.R.; resources, K.C.-M., N.D. and M.C.T.D.; data curation, K.C.-M., A.C.F.d.S. and S.M.R.; writing—original draft preparation, K.C.-M., A.C.F.d.S. and S.M.R.; writing—review and editing, K.C.-M., N.D., M.C.T.D., A.C.F.d.S., S.M.R. and G.N.; visualization, K.C.-M., N.D., M.C.T.D., A.C.F.d.S., S.M.R. and G.N.; supervision, K.C.-M.; project administration, K.C.-M. and A.C.F.d.S. All authors have read and agreed to the published version of the manuscript.

Funding: This study received a grant and a Research Grant from the São Paulo Research Foundation (Process no.: 2018/21769-4 and 2018/20593-0).

Institutional Review Board Statement: Not applicable.

Informed Consent Statement: Not applicable.

Data Availability Statement: Data are contained within the article.

Acknowledgments: We would like to thank Carlos Emilio Levy for providing us with bacterial samples and FAPESP (2018/21769-4 and 2018/20593-0) for their financial support and Espaço da Escrita—Pró-Reitoria de Pesquisa—UNICAMP—for the language services provided.

Conflicts of Interest: The authors declare no conflicts of interest.

Abbreviations

MRSA	Methicillin-resistant *Staphylococcus aureus*
Bio-AgNP	Biologically synthesized silver nanoparticles
AgNP	Silver nanoparticles
EDS	Energy Dispersive X-ray Spectroscopy
TEM	Transmission Electron Microscopy
SIM	Simvastatin
FICI	Fractional Inhibitory Concentration Index
WHO	World Health Organization
PBP2a	Penicillin-binding protein 2a
MRSA	Methicillin-resistant *Staphylococcus aureus*

HMG-CoA	3-hydroxy-3-methylglutaryl-CoenzymeA reductase
LDL	Low-density lipoprotein
DMSO	Dimethylsulfoxide
DLS	Dynamic light scattering
TSA	Tryptone Soy Agar
TSB	Tryptic Soy Broth
MIC	Minimum Inhibitory Concentration
CLSI	Clinical and Laboratory Standards Institute
MHB	Mueller Hinton Broth
OD	Optical density
TEM	Transmission Electron Microscopy
JCPDS	Joint Committee on Powder Diffraction Standards
XRD	X-ray Diffraction Spectroscopy
ATCC	American-Type Culture Collection

References

1. Hassoun, A.; Linden, P.K.; Friedman, B. Incidence, Prevalence, and Management of MRSA Bacteremia across Patient Populations—A Review of Recent Developments in MRSA Management and Treatment. *Crit. Care* **2017**, *21*, 211. [CrossRef] [PubMed]
2. Tacconelli, E.; Carrara, E.; Savoldi, A.; Harbarth, S.; Mendelson, M.; Monnet, D.L.; Pulcini, C.; Kahlmeter, G.; Kluytmans, J.; Carmeli, Y.; et al. Discovery, Research, and Development of New Antibiotics: The WHO Priority List of Antibiotic-Resistant Bacteria and Tuberculosis. *Lancet Infect. Dis.* **2018**, *18*, 318–327. [CrossRef] [PubMed]
3. WHO. *Global Report on Infection Prevention and Control*; WHO: Geneva, Switzerland, 2022; ISBN 9789240051164.
4. Lee, A.S.; de Lencastre, H.; Garau, J.; Kluytmans, J.; Malhotra-Kumar, S.; Peschel, A.; Harbarth, S. Methicillin-Resistant Staphylococcus Aureus. *Nat. Rev. Dis. Primers* **2018**, *4*, 18033. [CrossRef] [PubMed]
5. Fishovitz, J.; Hermoso, J.A.; Chang, M.; Mobashery, S. Penicillin-Binding Protein 2a of Methicillin-Resistant *Staphylococcus aureus*. *IUBMB Life* **2014**, *66*, 572–577. [CrossRef]
6. Kong, K.-F.; Schneper, L.; Mathee, K. Beta-Lactam Antibiotics: From Antibiosis to Resistance and Bacteriology. *APMIS* **2010**, *118*, 1–36. [CrossRef]
7. Abd El-Hamid, M.I.; El-Naenaeey, E.-S.Y.; Kandeel, T.M.; Hegazy, W.A.H.; Mosbah, R.A.; Nassar, M.S.; Bakhrebah, M.A.; Abdulaal, W.H.; Alhakamy, N.A.; Bendary, M.M. Promising Antibiofilm Agents: Recent Breakthrough against Biofilm Producing Methicillin-Resistant Staphylococcus Aureus. *Antibiotics* **2020**, *9*, 667. [CrossRef]
8. Cascioferro, S.; Carbone, D.; Parrino, B.; Pecoraro, C.; Giovannetti, E.; Cirrincione, G.; Diana, P. Therapeutic Strategies To Counteract Antibiotic Resistance in MRSA Biofilm-Associated Infections. *ChemMedChem* **2021**, *16*, 65–80. [CrossRef]
9. Silva, V.; Almeida, L.; Gaio, V.; Cerca, N.; Manageiro, V.; Caniça, M.; Capelo, J.L.; Igrejas, G.; Poeta, P. Biofilm Formation of Multidrug-Resistant MRSA Strains Isolated from Different Types of Human Infections. *Pathogens* **2021**, *10*, 970. [CrossRef]
10. Lebeaux, D.; Chauhan, A.; Rendueles, O.; Beloin, C. From in Vitro to in Vivo Models of Bacterial Biofilm-Related Infections. *Pathogens* **2013**, *2*, 288–356. [CrossRef]
11. Penesyan, A.; Gillings, M.; Paulsen, I. Antibiotic Discovery: Combatting Bacterial Resistance in Cells and in Biofilm Communities. *Molecules* **2015**, *20*, 5286–5298. [CrossRef]
12. Fayaz, A.M.; Balaji, K.; Girilal, M.; Yadav, R.; Kalaichelvan, P.T.; Venketesan, R. Biogenic Synthesis of Silver Nanoparticles and Their Synergistic Effect with Antibiotics: A Study against Gram-Positive and Gram-Negative Bacteria. *Nanomedicine* **2010**, *6*, 103–109. [CrossRef] [PubMed]
13. Patra, J.K.; Baek, K.-H. Antibacterial Activity and Synergistic Antibacterial Potential of Biosynthesized Silver Nanoparticles against Foodborne Pathogenic Bacteria along with Its Anticandidal and Antioxidant Effects. *Front. Microbiol.* **2017**, *8*, 167. [CrossRef] [PubMed]
14. Gimenez, I.F.; Anazetti, M.C.; Melo, P.S.; Haun, M.; De Azevedo, M.M.M.; Durán, N.; Alves, O.L. Cytotoxicity on V79 and HL60 Cell Lines by Thiolated-β-Cyclodextrin-Au/Violacein Nanoparticles. *J. Biomed. Nanotechnol.* **2005**, *1*, 352–358. [CrossRef]
15. Siddiqi, K.S.; Husen, A.; Rao, R.A.K. A Review on Biosynthesis of Silver Nanoparticles and Their Biocidal Properties. *J. Nanobiotechnol.* **2018**, *16*, 14. [CrossRef] [PubMed]
16. Durán, N.; Marcato, P.D.; Alves, O.L.; De Souza, G.I.; Esposito, E. Mechanistic Aspects of Biosynthesis of Silver Nanoparticles by Several Fusarium Oxysporum Strains. *J. Nanobiotechnol.* **2005**, *3*, 8. [CrossRef] [PubMed]
17. Figueiredo, E.; Ribeiro, J.; Nishio, E.; Scandorieiro, S.; Costa, A.; Cardozo, V.; de Oliveira, A.; Durán, N.; Panagio, L.; Kobayashi, R.; et al. New Approach For Simvastatin As An Antibacterial: Synergistic Effect With Bio-Synthesized Silver Nanoparticles Against Multidrug-Resistant Bacteria. *Int. J. Nanomed.* **2019**, *14*, 7975–7985. [CrossRef] [PubMed]
18. Foletto, V.S.; da Rosa, T.F.; Serafin, M.B.; Bottega, A.; Hörner, R. Repositioning of Non-Antibiotic Drugs as an Alternative to Microbial Resistance: A Systematic Review. *Int. J. Antimicrob. Agents* **2021**, *58*, 106380. [CrossRef] [PubMed]
19. Annamanedi, M.; Varma, G.Y.N.; Anuradha, K.; Kalle, A.M. Celecoxib Enhances the Efficacy of Low-Dose Antibiotic Treatment against Polymicrobial Sepsis in Mice and Clinical Isolates of ESKAPE Pathogens. *Front. Microbiol.* **2017**, *8*, 00805. [CrossRef]

20. Machado, C.d.S.; da Rosa, T.F.; Serafin, M.B.; Bottega, A.; Coelho, S.S.; Foletto, V.S.; Rampelotto, R.F.; Lorenzoni, V.V.; Marion, S.d.L.; Hörner, R. In Vitro Evaluation of the Antibacterial Activity of Amitriptyline and Its Synergistic Effect with Ciprofloxacin, Sulfamethoxazole–Trimethoprim, and Colistin as an Alternative in Drug Repositioning. *Med. Chem. Res.* **2020**, *29*, 166–177. [CrossRef]
21. Sankar, S.; Thangamalai, R.; Padmanaban, S.; Kannan, P.; Srinivasan, M.R.; Arunaman, C.S. In-Vitro Synergistic Antibacterial Effect of Atorvastatin and Ampicillin against Resistant *Staphylococcus* spp. and *E. coli* Isolated from Bovine Mastitis. *bioRxiv* **2019**. [CrossRef]
22. Ko, H.H.T.; Lareu, R.R.; Dix, B.R.; Hughes, J.D. Statins: Antimicrobial Resistance Breakers or Makers? *PeerJ* **2017**, *5*, e3952. [CrossRef]
23. Newman, C.B.; Preiss, D.; Tobert, J.A.; Jacobson, T.A.; Page, R.L.; Goldstein, L.B.; Chin, C.; Tannock, L.R.; Miller, M.; Raghuveer, G.; et al. Statin Safety and Associated Adverse Events A Scientific Statement from the American Heart Association. *Arterioscler. Thromb. Vasc. Biol.* **2019**, *39*, E38–E81. [CrossRef] [PubMed]
24. Khan, A.; Maki, K.C.; Ito, M.K.; Cohen, J.D.; Sponseller, C.A.; Bell, M.; Brinton, E.A.; Jacobson, T.A. Statin Associated Muscle Symptoms: Characteristics of Patients and Recommendations by Providers. *J. Clin. Lipidol.* **2015**, *9*, 460. [CrossRef]
25. Schech, S.; Graham, D.; Staffa, J.; Andrade, S.E.; La Grenade, L.; Burgess, M.; Blough, D.; Stergachis, A.; Chan, K.A.; Platt, R.; et al. Risk Factors for Statin-Associated Rhabdomyolysis. *Pharmacoepidemiol. Drug Saf.* **2007**, *16*, 352–358. [CrossRef] [PubMed]
26. Stoll, L.L.; McCormick, M.L.; Denning, G.M.; Weintraub, N.L. Antioxidant Effects of Statins. *Drugs Today* **2004**, *40*, 975. [CrossRef] [PubMed]
27. Tsubaki, M.; Fujiwara, D.; Takeda, T.; Kino, T.; Tomonari, Y.; Itoh, T.; Imano, M.; Satou, T.; Sakaguchi, K.; Nishida, S. The Sensitivity of Head and Neck Carcinoma Cells to Statins Is Related to the Expression of Their Ras Expression Status, and Statin-Induced Apoptosis Is Mediated via Suppression of the Ras/ERK and Ras/MTOR Pathways. *Clin. Exp. Pharmacol. Physiol.* **2017**, *44*, 222–234. [CrossRef] [PubMed]
28. Hsu, C.; Brahmandam, A.; Brownson, K.E.; Huynh, N.; Reynolds, J.; Lee, A.I.; Fares, W.H.; Ochoa Chaar, C.I. Statin Therapy Associated with Improved Thrombus Resolution in Patients with Deep Vein Thrombosis. *J. Vasc. Surg. Venous Lymphat. Disord.* **2019**, *7*, 169–175.e4. [CrossRef]
29. Li, G.; Zhao, J.; Li, B.; Zhang, X.; Ma, J.; Ma, X.; Liu, J. The Anti-Inflammatory Effects of Statins on Patients with Rheumatoid Arthritis: A Systemic Review and Meta-Analysis of 15 Randomized Controlled Trials. *Autoimmun. Rev.* **2018**, *17*, 215–225. [CrossRef]
30. Sheridan, A.; Wheeler-Jones, C.P.D.; Gage, M.C. The Immunomodulatory Effects of Statins on Macrophages. *Immuno* **2022**, *2*, 317–343. [CrossRef]
31. Jerwood, S.; Cohen, J. Unexpected Antimicrobial Effect of Statins. *J. Antimicrob. Chemother.* **2007**, *61*, 362–364. [CrossRef]
32. Graziano, T.S.; Cuzzullin, M.C.; Franco, G.C.; Schwartz-Filho, H.O.; de Andrade, E.D.; Groppo, F.C.; Cogo-Müller, K. Statins and Antimicrobial Effects: Simvastatin as a Potential Drug against Staphylococcus Aureus Biofilm. *PLoS ONE* **2015**, *10*, e0128098. [CrossRef] [PubMed]
33. de Carvalho, R.D.P.; Casarin, R.C.V.; de Lima, P.O.; Cogo-Müller, K. Statins with Potential to Control Periodontitis: From Biological Mechanisms to Clinical Studies. *J. Oral. Biosci.* **2021**, *63*, 232–244. [CrossRef] [PubMed]
34. Parolina de Carvalho, R.D.; de Andrade Moreno, J.; Roque, S.M.; Chan, D.C.H.; Torrez, W.B.; Stipp, R.N.; Bueno-Silva, B.; de Lima, P.O.; Cogo-Müller, K. Statins and Oral Biofilm: Simvastatin as a Promising Drug to Control Periodontal Dysbiosis. *Oral. Dis.* 2022, *ahead of print*. [CrossRef]
35. Sun, T.; Huang, J.; Zhang, W.; Zheng, X.; Wang, H.; Liu, J.; Leng, H.; Yuan, W.; Song, C. Simvastatin-Hydroxyapatite Coatings Prevent Biofilm Formation and Improve Bone Formation in Implant-Associated Infections. *Bioact. Mater.* **2023**, *21*, 44–56. [CrossRef] [PubMed]
36. Ansari, M.; Khan, H.; Khan, A.; Cameotra, S.; Alzohairy, M. Anti-Biofilm Efficacy of Silver Nanoparticles against MRSA and MRSE Isolated from Wounds in a Tertiary Care Hospital. *Indian J. Med. Microbiol.* **2015**, *33*, 101–109. [CrossRef] [PubMed]
37. Tarusha, L.; Paoletti, S.; Travan, A.; Marsich, E. Alginate Membranes Loaded with Hyaluronic Acid and Silver Nanoparticles to Foster Tissue Healing and to Control Bacterial Contamination of Non-Healing Wounds. *J. Mater. Sci. Mater. Med.* **2018**, *29*, 22. [CrossRef] [PubMed]
38. Lebeaux, D.; Ghigo, J.-M.; Beloin, C. Biofilm-Related Infections: Bridging the Gap between Clinical Management and Fundamental Aspects of Recalcitrance toward Antibiotics. *Microbiol. Mol. Biol. Rev.* **2014**, *78*, 510–543. [CrossRef] [PubMed]
39. Cluzet, V.C.; Gerber, J.S.; Nachamkin, I.; Metlay, J.P.; Zaoutis, T.E.; Davis, M.F.; Julian, K.G.; Royer, D.; Linkin, D.R.; Coffin, S.E.; et al. Duration of Colonization and Determinants of Earlier Clearance of Colonization with Methicillin-Resistant Staphylococcus Aureus. *Clin. Infect. Dis.* **2015**, *60*, 1489–1496. [CrossRef]
40. Durán, N.; Alves, O.L.; Esposito, E.; de Souza, G.I.; Marcato, P.D. Processo de Produção de Nanopartículas de Prata Estabilizadas por Proteínas na Produção de Produtos Têxteis Antibacterianos e o Tratamento dos Efluentes Produzidos. Braz. patent PI 0605681-4 A, 2006.
41. Kumar, S.A.; Ansary, A.A.; Ahmad, A.; Khan, M.I. Extracellular Biosynthesis of CdSe Quantum Dots by the Fungus, Fusarium Oxysporum. *J. Biomed. Nanotechnol.* **2007**, *3*, 190–194. [CrossRef]
42. CLSI. *Methods for Dilution Antimicrobial Susceptibility Tests for Bacteria That Grow Aerobically*, 11th ed.; Clinical and Laboratory Standards Institute: Malvern, PA, USA, 2018.

43. Odds, F.C. Synergy, Antagonism, and What the Chequerboard Puts between Them. *J. Antimicrob. Chemother.* **2003**, *52*, 1. [CrossRef]
44. Doern, C.D. When Does 2 Plus 2 Equal 5? A Review of Antimicrobial Synergy Testing. *J. Clin. Microbiol.* **2014**, *52*, 4124–4128. [CrossRef]
45. Wu, W.-S.; Chen, C.-C.; Chuang, Y.-C.; Su, B.-A.; Chiu, Y.-H.; Hsu, H.-J.; Ko, W.-C.; Tang, H.-J. Efficacy of Combination Oral Antimicrobial Agents against Biofilm-Embedded Methicillin-Resistant Staphylococcus Aureus. *J. Microbiol. Immunol. Infect.* **2013**, *46*, 89–95. [CrossRef] [PubMed]
46. Honary, S.; Barabadi, H.; Gharaei-Fathabad, E.; Naghibi, F. Green Synthesis of Silver Nanoparticles Induced by the Fungus Penicillium Citrinum. *Trop. J. Pharm. Res.* **2013**, *12*, 7–11. [CrossRef]
47. Birla, S.S.; Tiwari, V.V.; Gade, A.K.; Ingle, A.P.; Yadav, A.P.; Rai, M.K. Fabrication of Silver Nanoparticles by *Phoma glomerata* and Its Combined Effect against *Escherichia coli*, *Pseudomonas aeruginosa* and *Staphylococcus aureus*. *Lett. Appl. Microbiol.* **2009**, *48*, 173–179. [CrossRef] [PubMed]
48. Soni, N.; Prakash, S. Synthesis of Gold Nanoparticles by the Fungus Aspergillus Niger and Its Efficacy against Mosquito Larvae. *Rep. Parasitol.* **2012**, *2012*, 1–7. [CrossRef]
49. Vala, A.K.; Shah, S.; Patel, R.N. Biogenesis of Silver Nanoparticles by Marine- Derived Fungus Aspergillus Flavus from Bhavnagar Coast, Gulf of Khambhat, India. *J. Mar. Biol. Oceanogr.* **2014**, *3*, 1000122. [CrossRef]
50. Raj, S.; Chand Mali, S.; Trivedi, R. Green Synthesis and Characterization of Silver Nanoparticles Using Enicostemma Axillare (Lam.) Leaf Extract. *Biochem. Biophys. Res. Commun.* **2018**, *503*, 2814–2819. [CrossRef] [PubMed]
51. Baharara, J.; Ramezani, T.; Hosseini, N.; Mousavi, M. Silver Nanoparticles Synthesized Coating with Zataria Multiflora Leaves Extract Induced Apoptosis in HeLa Cells Through P53 Activation. *Iran. J. Pharm. Res.* **2018**, *17*, 627–639.
52. Noronha, V.T.; Paula, A.J.; Durán, G.; Galembeck, A.; Cogo-Müller, K.; Franz-Montan, M.; Durán, N. Silver Nanoparticles in Dentistry. *Dent. Mater.* **2017**, *33*, 1110–1126. [CrossRef]
53. Scandorieiro, S.; de Camargo, L.C.; Lancheros, C.A.C.; Yamada-Ogatta, S.F.; Nakamura, C.V.; de Oliveira, A.G.; Andrade, C.G.T.J.; Duran, N.; Nakazato, G.; Kobayashi, R.K.T. Synergistic and Additive Effect of Oregano Essential Oil and Biological Silver Nanoparticles against Multidrug-Resistant Bacterial Strains. *Front. Microbiol.* **2016**, *7*, 00760. [CrossRef]
54. Saeki, E.K.; Yamada, A.Y.; de Araujo, L.A.; Anversa, L.; Garcia, D.d.O.; de Souza, R.L.B.; Martins, H.M.; Kobayashi, R.K.T.; Nakazato, G. Subinhibitory Concentrations of Biogenic Silver Nanoparticles Affect Motility and Biofilm Formation in Pseudomonas Aeruginosa. *Front. Cell Infect. Microbiol.* **2021**, *11*, 656984. [CrossRef]
55. Bisignano, C.; Ginestra, G.; Smeriglio, A.; La Camera, E.; Crisafi, G.; Franchina, F.A.; Tranchida, P.Q.; Alibrandi, A.; Trombetta, D.; Mondello, L.; et al. Study of the Lipid Profile of ATCC and Clinical Strains of Staphylococcus Aureus in Relation to Their Antibiotic Resistance. *Molecules* **2019**, *24*, 1276. [CrossRef] [PubMed]
56. Habash, M.B.; Goodyear, M.C.; Park, A.J.; Surette, M.D.; Vis, E.C.; Harris, R.J.; Khursigara, C.M. Potentiation of Tobramycin by Silver Nanoparticles against Pseudomonas Aeruginosa Biofilms. *Antimicrob. Agents Chemother.* **2017**, *61*, e00415-17. [CrossRef]
57. Villa, F.; Remelli, W.; Forlani, F.; Gambino, M.; Landini, P.; Cappitelli, F. Effects of Chronic Sub-Lethal Oxidative Stress on Biofilm Formation by *Azotobacter vinelandii*. *Biofouling* **2012**, *28*, 823–833. [CrossRef] [PubMed]
58. Wang, L.; Hu, C.; Shao, L. The Antimicrobial Activity of Nanoparticles: Present Situation and Prospects for the Future. *Int. J. Nanomed.* **2017**, *12*, 1227–1249. [CrossRef] [PubMed]
59. Su, L.-J.; Zhang, J.-H.; Gomez, H.; Murugan, R.; Hong, X.; Xu, D.; Jiang, F.; Peng, Z.-Y. Reactive Oxygen Species-Induced Lipid Peroxidation in Apoptosis, Autophagy, and Ferroptosis. *Oxid. Med. Cell Longev.* **2019**, *2019*, 5080843. [CrossRef]
60. DIckey, S.W.; Cheung, G.Y.C.; Otto, M. Different Drugs for Bad Bugs: Antivirulence Strategies in the Age of Antibiotic Resistance. *Nat. Rev. Drug Discov.* **2017**, *16*, 457–471. [CrossRef]
61. Wang, C.C.; Yang, P.W.; Yang, S.F.; Hsieh, K.P.; Tseng, S.P.; Lin, Y.C. Topical Simvastatin Promotes Healing of Staphylococcus Aureus-Contaminated Cutaneous Wounds. *Int. Wound J.* **2016**, *13*, 1150–1157. [CrossRef]
62. Yılmaz; Özcengiz, G. Antibiotics: Pharmacokinetics, Toxicity, Resistance and Multidrug Efflux Pumps. *Biochem. Pharmacol.* **2017**, *133*, 43–62. [CrossRef]
63. Smelser, L.K.; Walker, C.; Burns, E.M.; Curry, M.; Black, N.; Metzler, J.A.; McDowell, S.A.; Bruns, H.A. Short Term, Low Dose Simvastatin Pretreatment Alters Memory Immune Function Following Secondary Staphylococcus Aureus Infection. *Curr. Pharm. Biotechnol.* **2016**, *17*, 886–893. [CrossRef]
64. Panáček, A.; Kvítek, L.; Smékalová, M.; Večeřová, R.; Kolář, M.; Röderová, M.; Dyčka, F.; Šebela, M.; Prucek, R.; Tomanec, O.; et al. Bacterial Resistance to Silver Nanoparticles and How to Overcome It. *Nat. Nanotechnol.* **2018**, *13*, 65–71. [CrossRef]
65. Bocate, K.P.; Reis, G.F.; de Souza, P.C.; Oliveira Junior, A.G.; Durán, N.; Nakazato, G.; Furlaneto, M.C.; de Almeida, R.S.; Panagio, L.A. Antifungal Activity of Silver Nanoparticles and Simvastatin against Toxigenic Species of Aspergillus. *Int. J. Food Microbiol.* **2019**, *291*, 79–86. [CrossRef] [PubMed]
66. Sahoo, J.; Sarkhel, S.; Mukherjee, N.; Jaiswal, A. Nanomaterial-Based Antimicrobial Coating for Biomedical Implants: New Age Solution for Biofilm-Associated Infections. *ACS Omega* **2022**, *7*, 45962–45980. [CrossRef] [PubMed]
67. Agnihotri, S.; Mukherji, S.; Mukherji, S. Immobilized Silver Nanoparticles Enhance Contact Killing and Show Highest Efficacy: Elucidation of the Mechanism of Bactericidal Action of Silver. *Nanoscale* **2013**, *5*, 7328. [CrossRef]
68. Roe, D.; Karandikar, B.; Bonn-Savage, N.; Gibbins, B.; Roullet, J.-B. Antimicrobial Surface Functionalization of Plastic Catheters by Silver Nanoparticles. *J. Antimicrob. Chemother.* **2008**, *61*, 869–876. [CrossRef] [PubMed]

69. Seymour, C. Audit of Catheter-Associated UTI Using Silver Alloy-Coated Foley Catheters. *Br. J. Nurs.* **2006**, *15*, 598–603. [CrossRef] [PubMed]
70. Pollini, M.; Paladini, F.; Catalano, M.; Taurino, A.; Licciulli, A.; Maffezzoli, A.; Sannino, A. Antibacterial Coatings on Haemodialysis Catheters by Photochemical Deposition of Silver Nanoparticles. *J. Mater. Sci. Mater. Med.* **2011**, *22*, 2005–2012. [CrossRef] [PubMed]
71. Mussin, J.; Robles-Botero, V.; Casañas-Pimentel, R.; Rojas, F.; Angiolella, L.; San Martín-Martínez, E.; Giusiano, G. Antimicrobial and Cytotoxic Activity of Green Synthesis Silver Nanoparticles Targeting Skin and Soft Tissue Infectious Agents. *Sci. Rep.* **2021**, *11*, 14566. [CrossRef]
72. Orta-García, S.T.; Plascencia-Villa, G.; Ochoa-Martínez, A.C.; Ruiz-Vera, T.; Pérez-Vázquez, F.J.; Velázquez-Salazar, J.J.; Yacamán, M.J.; Navarro-Contreras, H.R.; Pérez-Maldonado, I.N. Analysis of Cytotoxic Effects of Silver Nanoclusters on Human Peripheral Blood Mononuclear Cells ' in Vitro'. *J. Appl. Toxicol.* **2015**, *35*, 1189–1199. [CrossRef]
73. Alves, M.F.; Paschoal, A.C.C.; Klimeck, T.D.F.; Kuligovski, C.; Marcon, B.H.; de Aguiar, A.M.; Murray, P.G. Biological Synthesis of Low Cytotoxicity Silver Nanoparticles (AgNPs) by the Fungus Chaetomium Thermophilum—Sustainable Nanotechnology. *J. Fungi* **2022**, *8*, 605. [CrossRef]
74. Haidari, H.; Kopecki, Z.; Bright, R.; Cowin, A.J.; Garg, S.; Goswami, N.; Vasilev, K. Ultrasmall AgNP-Impregnated Biocompatible Hydrogel with Highly Effective Biofilm Elimination Properties. *ACS Appl. Mater. Interfaces* **2020**, *12*, 41011–41025. [CrossRef]
75. Chang, C.T.; Chen, Y.T.; Hsieh, Y.K.; Girsang, S.P.; Wang, R.S.; Chang, Y.C.; Shen, S.H.; Shen, C.R.; Lin, T.P.; Wan, D.; et al. Dual-Functional Antibiofilm Polymer Composite for Biodegradable Medical Devices. *Mater. Sci. Eng. C* **2021**, *123*, 111985. [CrossRef] [PubMed]
76. Mehregan, D.R.; Mehregan, D.A.; Pakideh, S. Cheilitis Due to Treatment with Simvastatin. *Cutis* **1998**, *62*, 197–198. [PubMed]
77. Vasconcelos, O.M.; Campbell, W.W. Dermatomyositis-like Syndrome and HMG-CoA Reductase Inhibitor (Statin) Intake. *Muscle Nerve* **2004**, *30*, 803–807. [CrossRef] [PubMed]
78. Noël, B. Lupus Erythematosus and Other Autoimmune Diseases Related to Statin Therapy: A Systematic Review. *J. Eur. Acad. Dermatol. Venereol.* **2007**, *21*, 17–24. [CrossRef] [PubMed]
79. Abadir, R.; Liebmann, J. Clinical Oncology Case Report Radiation Reaction Recall Following Simvastatin Therapy: A New Observation. *Clin. Oncol.* **1995**, *7*, 325–326. [CrossRef] [PubMed]
80. Field, S.; Bourke, B.; Hazelwood, E.; Bourke, J.F. Simvastatin-Occupational Contact Dermatitis. *Contact Dermat.* **2007**, *57*, 282–283. [CrossRef]
81. Peramiquel, L.; Serra, E.; Dalmau, J.; Vila, A.T.; Mascaró, J.M.; Alomar, A. Occupational Contact Dermatitis from Simvastatin. *Contact Dermat.* **2005**, *52*, 286–287. [CrossRef]
82. Holme, S.A.; Pearse, A.D.; Anstey, A.V. Chronic Actinic Dermatitis Secondary to Simvastatin. *Photodermatol. Photoimmunol. Photomed.* **2002**, *18*, 313–314. [CrossRef]
83. Oskay, T.; Kutluay, L. Acute Generalized Exanthematous Pustulosis Induced by Simvastatin. *Clin. Exp. Dermatol.* **2003**, *28*, 558–559. [CrossRef]
84. Stoebner, P.-E.; Michot, C.; Ligeron, C.; Durand, L.; Meynadier, J.; Meunier, L. Simvastatin-Induced Lichen Planus Pemphigoides. *Ann. Dermatol. Venereol.* **2003**, *130*, 187–190.